All-fiber few-mode erbium-doped fiber amplifier supporting six spatial modes

Zhenzhen Zhang (张振振)[1], Cheng Guo (郭 骋)[1], Liang Cui (崔 亮)[1], Yichi Zhang (张一弛)[2], Cheng Du (杜 城)[2], and Xiaoying Li (李小英)[1,*]

[1]*Key Laboratory of Opto-electronic Information Technical Science of Ministry of Education, College of Precision Instruments and Opto-electronics Engineering, Tianjin University, Tianjin 300072, China*

[2]*Fiberhome & Fujikura Optics Co., Ltd., Wuhan 430074, China*

**Corresponding author: xiaoyingli@tju.edu.cn*

Received April 28, 2019; accepted August 22, 2019; posted online September 5, 2019

Using the few-mode erbium-doped fiber (FM-EDF) with a simple two-layer erbium-doped structure, we demonstrate an all-fiber FM-EDF amplifier. The gain equalization among the six spatial modes supported by the FM-EDF is achieved when only the pump in the fundamental mode (LP_{01}) is applied. When the signals in six spatial modes are simultaneously amplified, the average modal gain is about 15 dB, and differential modal gain is about 2.5 dB for the signal at 1550 nm.

OCIS codes: 060.2330, 060.4230, 060.2410, 140.4480.

doi: 10.3788/COL201917.100604.

Space division multiplexing is a promising technology to break through the capacity crunch of a single-mode fiber (SMF) optical network[1]. Recent years have seen the growing interest in studying mode division multiplexing (MDM) by using different spatial modes to carry different data information[2–4]. For the long-haul MDM transmission system, the few-mode erbium-doped fiber amplifiers (FM-EDFAs) will be a key block to compensate for the fiber transmission loss[5]. Since the high differential modal gain (DMG) can result in the MDM system outage, the ability to obtain modal gain equalization among all modes supported by the few-mode erbium-doped fiber (FM-EDF) is critical[6].

The DMG of the FM-EDFA is originated from the different overlap integral between signal-mode intensity, pump-mode intensity, and erbium-doped distribution in the FM-EDF. In general, DMG can be controlled by properly designing the erbium dopant profile[7,8] and by configurating the intensity distribution of the pump beam[9–11]. A cladding pump is another solution to achieve gain equalized FM-EDFA, but with a cost of low pump efficiency[12].

So far, a lot of experiments have successfully demonstrated FM-EDFAs. However, most of the core-pumped FM-EDFAs were based on the bulky free-space component[13]. To make the FM-EDFAs more practical, in addition to better designing the working principle to reduce the complexity of FM-EDFAs, minimizing the components is also important.

In this Letter, we study the core-pumped FM-EDFA, whose conversion efficiency is much higher than the cladding-pumped one[14]. By using one piece of FM-EDF with a two-layer erbium-doped structure[15], we experimentally demonstrate a gain equalized FM-EDFA supporting six spatial modes when only the fundamental mode (LP_{01}) pump is applied. Compared with the six-mode FM-EDFA[10,11], realized by launching two degenerate LP_{21} pump modes into the FM-EDF with a uniformly doped profile, the pump configuration of our FM-EDFA is simpler. Moreover, our FM-EDFA is an all-fiber device and has the potential for inline application.

The experimental setup is shown in Fig. 1. Our FM-EDFA consists of two few-mode homemade wavelength multiplexers (HWMs) with 1.85 m FM-EDF spliced in between. Each HWM is realized by respectively coupling the three ports of a dichroic mirror (DM) with few-mode fiber (FMF1), FMF2, and a 980 nm SMF, as shown in the inset of Fig. 1. Similar to the commercially available SMF wavelength division multiplexer, the HWM is sealed in a tube with the diameter and length of 5.5 and 38 mm, respectively. The insertion losses of the HWM for signals in six spatial modes, LP_{01}, LP_{11o}, LP_{11e}, LP_{21o}, LP_{21e}, and LP_{02}, are 0.40 dB, 0.64 dB, 0.78 dB, 0.77 dB, 0.87 dB, and 1.59 dB, respectively. While for the pump in LP_{01}, the insertion loss is about 0.96 dB. HWM1 is used to combine the input signals of six spatial modes and LP_{01} pump. The input signals in different spatial modes are amplified by the LP_{01} pump in the FM-EDF. By passing the output of the FM-EDF through HWM2, the residual pump is isolated, and the amplified signals are extracted out. The input signals in six different spatial modes are obtained by sending the output of a tunable laser (Santec ECL210) with the linewidth of about 200 MHz into different ports of a mode selective photonic lantern (MSPL)[16], which functions as a mode converter and combiner. To avoid the interference between different spatial modes, delay lines (DLs) are added in each input of the MSPL. The fiber lengths used to introduce delay in each port are 8 m, 25 m, 31 m, 100 m, and 200 m, respectively, which are all greater than the coherence length of 0.48 m (determined by the 200 MHz linewidth of the laser). Moreover, we place fiber polarization controllers (FPCs) in each

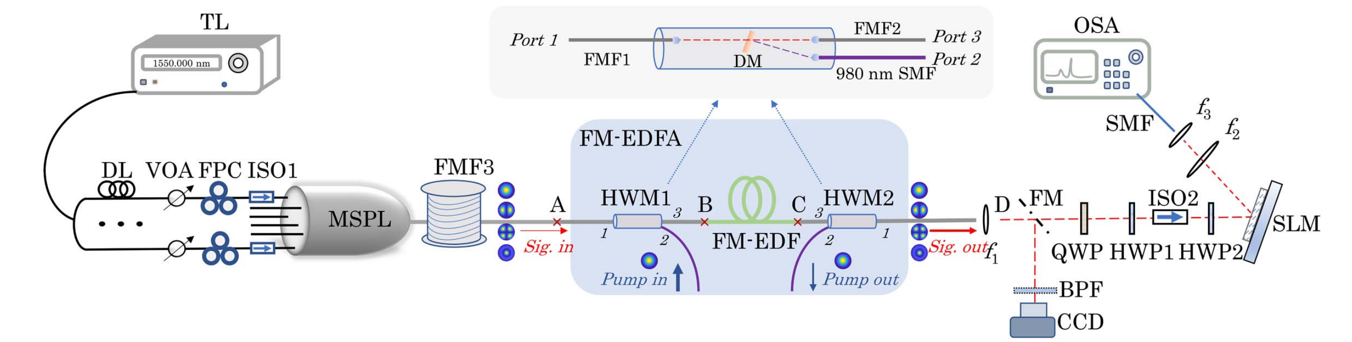

Fig. 1. Experimental setup. TL, tunable lase; DL, delay; VOA, variable optical attenuator; FPC, fiber polarization controller; ISO, isolator; MSPL, mode selective photonic lantern; FMF, few-mode fiber; HWM, homemade wavelength multiplexer; FM-EDF, few-mode erbium-doped fiber; FM, flip mirror; BPF, bandpass filter; CCD, coupled charge device; QWP, quarter-wave plate; HWP, half-wave plate; SLM, spatial light modulator; SMF, single-mode fiber; OSA, optical spectrum analyzer; f_1, f_2, and f_3, lenses with focal lengths of 11 mm, 300 mm, and 3.1 mm, respectively; DM, dichroic mirror. The inset shows the configuration of the HWM, which is sealed in a tube with the diameter and length of 5.5 and 38 mm. The dashed lines denote the free-space transmission.

input of the MSPL to ensure the purity of the converted mode, since the performance of the MSPL is wavelength and polarization dependent. To mimic the inline transmission, the signals then pass through a 20 m FMF3. FMF1–FMF3 (OFS Optics #35275) are all step index fibers supporting six spatial modes, including LP_{01}, $LP_{11o(e)}$, $LP_{21o(e)}$, and LP_{02}. The performance of the FM-EDFA is analyzed by using an optical spectrum analyzer (OSA) when the output of HWM2 is demultiplexed with a programmed spatial light modulator (SLM) (Holoeye Pluto HES 6010). To ensure the amplification process is not disturbed by the reflection light, polarization independent isolators are placed at each signal input port of the MSPL. Moreover, the output end of HWM2 is cut at the angel of 8°, and polarization dependent isolators in combination with a quarter-wave plate (QWP) and a half-wave plate (HWP1) are used to further reduce the back-propagation light. HWP2 is used to rotate the polarization state of the amplified signal so that it is reflected by the SLM with high efficiency.

The FM-EDF supporting six spatial modes is fabricated by modified chemical vapor deposition and a chelate delivery system technique. The core diameter of the FM-EDF is 20 μm, and its NA is about 0.12. Figures 2(a) and 2(b) plot its cross section, the profile of relative refractive index and erbium ion concentration, respectively.

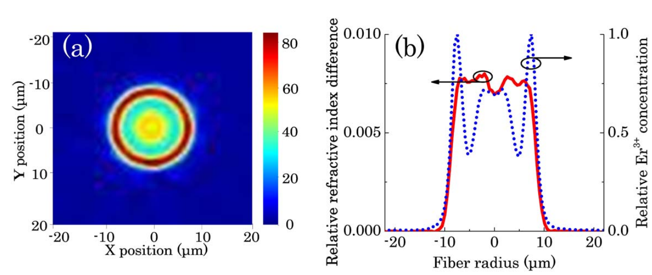

Fig. 2. (a) Cross section of the erbium ions and (b) the profile of the relative refractive index and erbium ion concentration in the FM-EDF.

Indeed, this FM-EDF is fabricated according to the design in Ref. [15]. However, due to the ion diffusion effect and other imperfections during the fabrication process, erbium ion distribution is different from the original design, and the profile of the erbium ions seems like the 'batman' profile[7]. One sees that the erbium-doped distribution has a simple two-layer structure. The erbium ion concentration in the outer layer is higher than that in the inner. In this case, overlap integrals between the signal intensities in different spatial modes, LP_{01} pump intensity, and erbium-doped distribution are about the same. Hence, the gain equalized amplification using the 980 nm pump in LP_{01} can be achieved[15].

We first verify the modal property of the 980 nm pump. The experiment is carried out in the process of splicing the two HWMs with the FM-EDF. The pump is launched from port 2 of HWM1, and the input signals are blocked. Figures 3(a) and 3(b) display the modal patterns of pump at the input and output of the FM-EDF, respectively. Figure 3(a), directly obtained by observing the attenuated pump light at port 3 of HWM1 (point B in Fig. 1) with an InGaAs coupled charge device (CCD), indicates that input pump is still in LP_{01} after being reflected by the DM and transmitting through FMF2 in HWM1. Figure 3(b), recorded by CCD after placing a DM at the output of the FM-EDF (point C in Fig. 1) to get rid of the influence of amplified spontaneous emission (ASE), manifests that the pump is propagating in the FM-EDF along its LP_{01}.

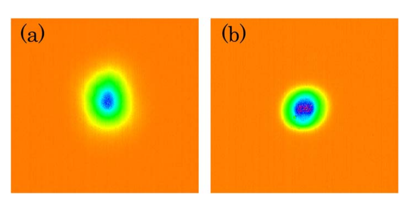

Fig. 3. Modal patterns of the 980 nm pump at the (a) input and (b) output of the FM-EDF, respectively.

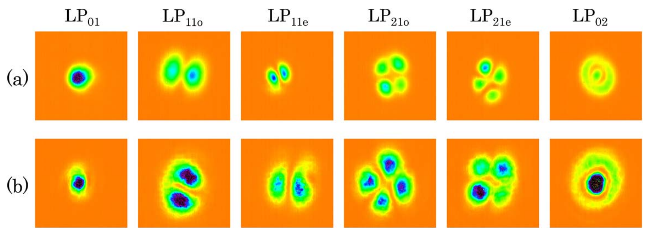

Fig. 4. Modal patterns of the signals in different spatial modes measured at the (a) input and (b) output ports of the FM-EDFA, respectively. The wavelength of the signal is 1550 nm.

During the splicing process, we also characterize the modal property of signals at the input and output of the FM-EDFA (see points A and D in Fig. 1), respectively, by using the CCD. In the experiment, a 1550 nm signal successively in different spatial modes (LP_{01}, $LP_{11o(e)}$, $LP_{21o(e)}$, and LP_{02}) and LP_{01} pump is presented in port 1 and port 2 of HWM1, respectively. Figure 4(a) shows the patterns of input signals in different spatial modes. The amplified signals in Fig. 4(b) are obtained by passing the output of HWM2 through a bandpass filter, which is centered at 1550 nm with a 3 dB bandwidth of about 12 nm. Comparing Figs. 4(a) and 4(b), one sees that the modal purity of signals is well preserved when input signals are amplified by the FM-EDF. There is no obvious mode coupling between different mode groups, because we have carefully optimized the splicing between the FMF and EDF to reduce mode mismatch. In general, the modal pattern of the output is a combination of the degenerated modes due to mode coupling. However, the output modal pattern varies with the polarization of input signal. For the signal with a specific polarization state, the output mode pattern (such as pure LP_{11o}) with no obvious degenerate mode coupling effect can be achieved. Considering the signals in different spatial modes can be decoded by using a multiple input multiple output (MIMO) algorithm even if there are mode coupling effects in the transmission process[8], the polarization of our input signal in different spatial modes is carefully chosen so that there is no obvious degenerate mode coupling effect for the amplified output of the FM-EDF. By doing so, we can clearly demonstrate the performance of our FM-EDFA.

Before characterizing the FM-EDFA with signals in six spatial modes simultaneously injected, we test the performance of the SLM, which functions as a mode demultiplexer. In this experiment, signals with different spatial modes are sequentially launched from different ports of the MSPL, and the pump power is fixed at 100 mW. Since the input signal modes are linearly polarized and specially arranged to minimize the mode coupling in FM-EDF, the amplified signal in each spatial mode has good modal purity, and the degree of its polarization is close to the ideal. For each kind of signal mode, the SLM is successively programmed to demultiplex the modes supported by the FM-EDF, including the LP_{01}, $LP_{11o(e)}$, $LP_{21o(e)}$, and LP_{02} modes. After coupling the demultiplexed mode into the LP_{01} and coupling it into a piece of SMF, we then deduce the crosstalk between different spatial modes by measuring and comparing the powers obtained in different cases. In each set of measurements, the powers out of the SMF are normalized by the value (see the diagonal elements in Table 1), which is obtained when the SLM is programmed to convert the signal mode into the LP_{01}. The measurement results for input signals in six spatial modes are shown in Table 1. One sees that the crosstalk effect for the LP_{01} signal is the lowest. For signals in higher-order spatial modes, the crosstalk performance is slightly degraded due to the subtle distortion of the modal pattern for the amplified signal (see Fig. 4). However, in almost all cases, the isolations between different spatial modes are better than 10 dB. The crosstalk effect of the demultiplexer realized by properly programming the SLM is slightly high, because the non-ideal MSPL crosstalk is measured to be up to −9 dB. If mode multiplexers with negligible crosstalk effect were available[17,18], the value in Table 1 would be significantly reduced. On the other hand, even if the crosstalk stays at the current level, the signal quality will not be damaged, since the MIMO technique can still be used to demultiplex the signal in each mode[19].

Table 1. Crosstalk Effect When the SLM is Programed to Convert Different Spatial Modes into LP_{01} (in dB)

		IM-MSPL[a]					
		LP_{01}	LP_{11o}	LP_{11e}	LP_{21o}	LP_{21e}	LP_{02}
MD-SLM[b]	LP_{01}	0	−20.00	−18.94	−16.85	−15.16	−18.70
	LP_{11o}	−11.84	0	−12.01	−14.64	−13.80	−12.18
	LP_{11e}	−10.71	−8.86	0	−12.52	−12.22	−11.55
	LP_{21o}	−10.73	−10.76	−10.18	0	−11.73	−13.57
	LP_{21e}	−10.41	−11.02	−8.11	−9.90	0	−10.68
	LP_{02}	−9.06	−13.13	−5.87	−12.53	−9.85	0

[a]IM-MSPL, input mode of the MSPL.
[b]MD-SLM, mode demultiplexed by SLM.

We then characterize the modal gain and noise figure (NF) of our FM-EDFA. The length of the FM-EDF is about 1.85 m, at which the higher gain and lower NF are achieved simultaneously. In this experiment, we simultaneously inject signals into each input port of the MSPL, so that signals in six different spatial modes are simultaneously injected into the FM-EDF. The power of the signal in each mode at the input of the FM-EDF is fixed at 50 μW. This is achieved by properly adjusting the variable optical attenuator (VOA) at each input port of the MSPL and after taking the insertion loss of the MSPL and splicing loss into account. By optimizing the fusion-taper technique, the splicing loss for the signals from the six input ports of the MSPL to the output of HWM1 in six spatial modes, LP_{01}, LP_{11o}, LP_{11e}, LP_{21o}, LP_{21e}, and LP_{02}, are 4.6 dB, 4.3 dB, 5.4 dB, 5.5 dB, 4.7 dB, and 7.9 dB, respectively. When the simultaneously amplified signals are measured at the output of HWM2, we successively demultiplex each mode by converting it to the LP_{01} with the programmed SLM. Moreover, in each measurement, the signal and noise powers measured by the OSA are corrected by the transmission efficiency between the output of HWM2 and input of the OSA.

The NF (in dB) of the ith mode is deduced by the equation[20]

$$\mathrm{NF}_i = 10\log_{10}\left(\frac{1}{G_i} + \frac{P_{ASE\_i}}{h\nu_s G_i \Delta\nu}\right), \tag{1}$$

where $G_i = \frac{P_i}{P_{in\_i}}$, with P_{in_i} and P_i, respectively, denoting the powers of input and output signals in the ith mode, is the modal gain of the ith mode (linear units). P_{ASE_i} is the power of the ASE in the ith mode within the bandwidth $\Delta\nu$, h is Planck's constant, and ν_s is the signal optical frequency. In the experiment, to deduce the key parameters in Eq. (1), P_i and P_{ASE_i}, both powers of the signal and ASE in each mode, are measured. Moreover, since the powers of the signal and ASE in the ith mode and other modes will couple with each other via crosstalk, the directly measured power needs to be corrected. For example, the corrected power of the signal in the ith mode is

$$P_i = P_{i'} - \sum_n X_{in} \cdot P_{i'} + \sum_n X_{ni} \cdot P_n, \tag{2}$$

where $P_{i'}$ is the directly measured power in the ith mode, and P_n is the power directly measured in the nth mode. X_{in} is the crosstalk degree describing signal input in the ith mode but with the output coupled to the nth mode, X_{ni} is the crosstalk degree describing signal in the nth mode but with the output coupled to the ith mode. The values of X_{in} and X_{ni} are listed in Table 1. Using a similar method and procedure, we can correct the crosstalk effect and retrieval of the power of ASE in the ith mode.

Figures 5(a) and 5(b) demonstrate the modal gains and the NFs for signals in each spatial mode measured by varying the pump power. It is clear that for the signal in each spatial mode, the modal gains increase with the pump

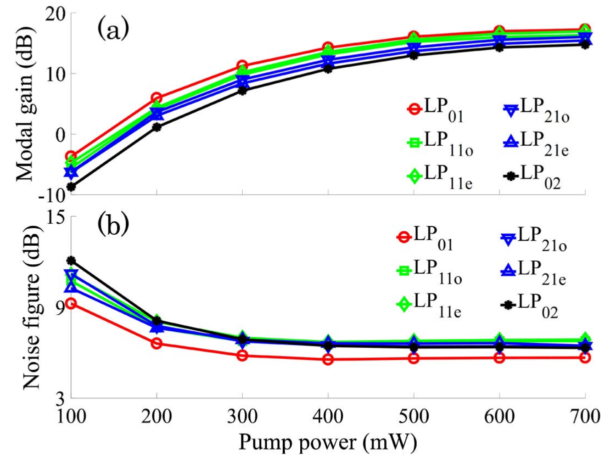

Fig. 5. (a) Modal gains and (b) NFs for the signal in different spatial modes as a function of the pump power. The results are corrected by taking the crosstalk effect into account. In the measurement, the signal wavelength is 1550 nm.

power in the beginning and start to saturate when the pump power is greater than 400 mW. When the pump power is about 550 mW, the average modal gains for all six spatial modes supported by the FM-EDF are about 15 dB. We find that the DMG among all spatial modes is about 2.5 dB. For each mode, the NFs decrease with the increase of the pump and tend to a constant. One sees that the NF for signals in the LP_{01} is the lowest and tends to 5 dB for high pump power. For signals in higher-order modes, their corresponding NFs are all higher than that of the LP_{01}. This is because the erbium ion concentration in the outer layer of the FM-EDF is higher than that in the inner layer. So, the LP_{01} pump mode might result in a higher ASE power for signals in higher-order spatial modes[21]. However, different from using a higher-order spatial mode pump, the LP_{01} pumped FM-EDFA does not exhibit an angular dependence on gain and NF[9]. Therefore, although the usage of pump in only the LP_{01} greatly simplifies the pump configuration and eliminates the angular dependence of gain and NF, the trade-off for realizing the modal gain equalization is the increased NF for the higher-order spatial mode.

To evaluate the gain and NF performance of the FM-EDFA across the C band, we repeat the measurement in Fig. 5 by changing the wavelength of the input signal from 1530 to 1565 nm with a step of 5 nm. Figures 6(a) and 6(b) plot the modal gains and NFs as a function of signal wavelength after correcting the crosstalk effect. In the experiment, the pump power is fixed at 550 mW. From Fig. 6(a), we find that the average modal gain across the C band is about 15 dB. The highest gain corresponds to the wavelength of about 1530 nm, however, the absorption coefficient of the erbium-doped fiber (EDF) and noise of the EDF amplifier (EDFA) at this wavelength are also the highest, which is similar to the case in the single-mode EDF. Although the gain excursion over the whole C band for the different modes is about 6 dB, the gain for the

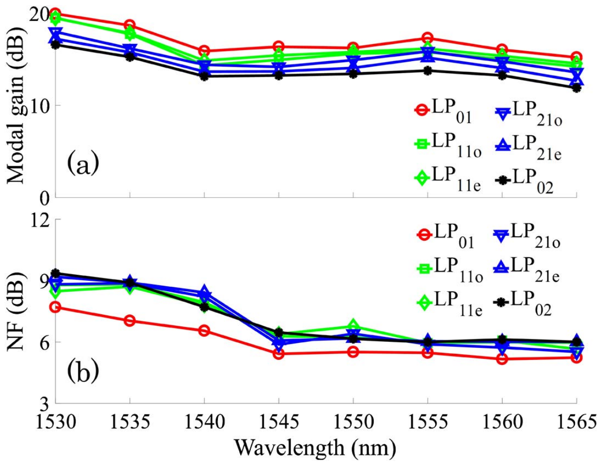

Fig. 6. (a) Modal gains and (b) NFs for the signal in different spatial modes as a function of signal wavelength. The results are corrected by taking the crosstalk effect into account. In the experiment, the pump power is fixed at 550 mW.

signal is quite constant, and the gain excursion is less than 3.5 dB for each spatial mode in the wavelength range of 1540–1565 nm. The DMGs vary with signal wavelength, but it is less than 3.5 dB for a fixed signal wavelength. From Fig. 6(b), we find that the NFs of the amplified signals in the six spatial modes are less than 8 dB in the wavelength range of 1540–1565 nm. For the fixed signal wavelength, the difference of NFs between different spatial modes is about 2 dB. While for a fixed spatial mode, the ripple of the NF is about 4 dB in the wavelength range of 1540–1565 nm.

In conclusion, we demonstrated an all-fiber FM-EDFA, which supports six spatial modes and is suitable for inline amplification. Using the FM-EDF with a simple two-layer erbium-doped structure, the gain equalization is achieved when only the pump in LP_{01} is applied. When the 1550 nm signals in six spatial modes are simultaneously amplified, the average modal gain is about 15 dB, and DMG is lower than 2.5 dB. We expect to further improve the performance of the FM-EDFA by optimizing the fabrication process to reduce the deviation between the parameters of the fabricated FM-EDF and designed ones[15].

This work was supported by the National Basic Research Program of China (No. 2014CB340103/01).

References

1. D. J. Richardson, J. M. Fini, and L. E. Nelson, Nat. Photon. **7**, 354 (2013).
2. G. Li, N. Bai, N. Zhao, and C. Xia, Adv. Opt. Photon. **6**, 413 (2014).
3. Z. Li, D. Lu, B. Zuo, S. Liang, X. Zhou, and J. Pan, Chin. Opt. Lett. **14**, 080601 (2016).
4. J. Xing, J. Wen, J. Wang, F. Pang, Z. Chen, Y. Liu, and T. Wang, Chin. Opt. Lett. **16**, 100604 (2018).
5. P. M. Krummrich, in *Optical Fiber Communication Conference and Exposition* (2012), paper OW1D.1.
6. K.-P. Ho and J. M. Kahn, Opt. Express **19**, 16612 (2011).
7. Q. Kang, E.-L. Lim, Y. Jung, J. K. Sahu, F. Poletti, C. Baskiotis, S.-u. Alam, and D. J. Richardson, Opt. Express **20**, 20835 (2012).
8. E. Ip, M. Li, K. Bennett, Y. Huang, A. Tanaka, A. Korolev, K. Koreshkov, W. Wood, E. Mateo, J. Hu, and Y. Yano, J. Lightwave Technol. **32**, 790 (2014).
9. N. Bai, E. Ip, T. Wang, and G. Li, Opt. Express **19**, 16601 (2011).
10. Y. Jung, Q. Kang, J. K. Sahu, B. Corbett, J. O'Callagham, F. Poletti, S.-U. Alam, and D. J. Richardson, IEEE Photon. Technol. Lett. **26**, 1100 (2014).
11. G. Lopez-Galmiche, Z. Sanjabi Eznaveh, J. E. Antonio-Lopez, A. M. Velazquez Benitez, J. Rodriguez Asomoza, J. J. Sanchez Mondragon, C. Gonnet, P. Sillard, G. Li, A. Schulzgen, C. M. Okonkwo, and R. Amezcua Correa, Opt. Lett. **41**, 2588 (2016).
12. Z. Zhang, C. Guo, L. Cui, Q. Mo, N. Zhao, C. Du, X. Li, and G. Li, Opt. Lett. **43**, 1550 (2018).
13. Y. Jung, S. U. Alam, and D. J. Richardson, in *Optical Fiber Communication Conference*, OSA Technical Digest (2018), paper M4D.3.
14. Y. Jung, S.-U. Alam, and D. J. Richardson, *Handbook of Optical Fibers* (Springer, 2018).
15. Q. Zhao, Z. Zhang, N. Zhao, and X. Li, Laser Optoelectron. Progress **53**, 030602 (2016).
16. A. M. Velazquez-Benitez, J. C. Alvarado, G. Lopez-Galmiche, J. E. Antonio-Lopez, J. Hernández-Cordero, J. Sanchez-Mondragon, P. Sillard, C. M. Okonkwo, and R. Amezcua-Correa, Opt. Lett. **40**, 1663 (2015).
17. N. Barre, B. Denolle, P. Jian, J. Morizur, and G. Labroille, in *2017 Optical Fiber Communications Conference and Exhibition (OFC)* (2017), paper Th2A.7.
18. D. Ge, Y. Gao, Y. Yang, L. Shen, Z. Li, Z. Chen, Y. He, and J. Li, Opt. Commun. **451**, 97 (2019).
19. P. J. Winzer, A. H. Gnauck, A. Konczykowska, F. Jorge, and J. Y. Dupuy, in *37th European Conference and Exposition on Optical Communications*, OSA Technical Digest (CD) (2011), paper Tu.5.B.7.
20. P. M. Becker, A. A. Olsson, and J. R. Simpson, *Erbium-Doped Fiber Amplifiers: Fundamentals and Technology* (Elsevier, 1999).
21. P. Genevaux, C. Simonneau, G. Le Cocq, Y. Quiquempois, L. Bigot, A. Boutin, and G. Charlet, J. Lightwave Technol. **34**, 456 (2016).